



# *Vibrio cholerae* hemolysin: The $\beta$ -trefoil domain is required for folding to the native conformation



Amarshi Mukherjee, Sreerupa Ganguly, Nabendu S. Chatterjee, Kalyan K. Banerjee\*

Division of Biochemistry, National Institute of Cholera and Enteric Diseases, Kolkata 700 010, India

## ARTICLE INFO

### Article history:

Received 9 August 2016

Received in revised form

4 September 2016

Accepted 17 September 2016

Available online 22 September 2016

### Keywords:

*Vibrio cholerae* hemolysin

$\beta$ -Pore-forming toxin

$\beta$ -Trefoil domain

$\beta$ -Prism lectin domain

Protein folding

## ABSTRACT

*Vibrio cholerae* cytotoxin/hemolysin (VCC) is a 65 kDa  $\beta$ -pore-forming toxin causing lysis and death of eukaryotic cells. Apart from the core cytotoxin domain, VCC has two lectin domains with  $\beta$ -trefoil and  $\beta$ -prism folds. The  $\beta$ -prism domain binds to cell surface carbohydrate receptors; the role of the  $\beta$ -trefoil domain is unknown. Here, we show that the pro-VCC mutant without the  $\beta$ -trefoil domain formed aggregates highly susceptible to proteolysis, suggesting lack of a properly folded compact structure. The VCC variants with Trp532Ala or Trp534Ala mutation in the  $\beta$ -trefoil domain formed hemolytically inactive, protease-resistant, ring-shaped SDS-labile oligomers with diameters of  $\sim 19$  nm. The Trp mutation induced a dramatic change in the global conformation of VCC, as indicated by: (a) the change in surface polarity from hydrophobic to hydrophilic; (b) movement of core Trp residues to the protein-water interface; and (c) decrease in reactivity to the anti-VCC antibody by  $> 100$ -fold. In fact, the mutant VCC had little similarity to the wild toxin. However, the association constant for the carbohydrate-dependent interaction mediated by the  $\beta$ -prism domain decreased marginally from  $\sim 3 \times 10^8$  to  $\sim 5 \times 10^7$  M $^{-1}$ . We interpret the observations by proposing: (a) the  $\beta$ -trefoil domain is critical to the folding of the cytotoxin domain to its active conformation; (b) the  $\beta$ -prism domain is an autonomous folding unit.

© 2016 The Authors. Published by Elsevier B.V. This is an open access article under the CC BY-NC-ND license (<http://creativecommons.org/licenses/by-nc-nd/4.0/>).

## 1. Introduction

*Vibrio cholerae* cytotoxin/hemolysin VCC; [1–3] is a  $\beta$ -pore-forming toxin  $\beta$ -PFT; [4–6] that causes colloid osmotic hemolysis of mammalian erythrocytes and apoptosis of epithelial and immune cells by forming 14-stranded heptameric  $\beta$ -barrel diffusion channels of diameter  $\sim 1$  nm in the plasma membrane bilayer [7–9]. VCC, expressed by virtually all *V. cholerae* El Tor O1 and non-O1 strains [10], is released into the growth medium as the inactive precursor, 79 kDa pro-VCC. The mature 65 kDa VCC is generated by removal of the 15 kDa N-terminus Pro-domain by endogenous or exogenous proteases at a site in the 15-residue cleavage motif of the 29-residue flexible linker joining the domain to the N-terminus of the cytotoxin domain [11]. The exact site of the cleavage depends on the specificity of the protease. VCC is considered a major accessory virulence factor of *V. cholerae* [10,12].

The analysis of the amino acid sequence [2] and X-ray crystallography [13] revealed that the  $\sim 725$ -residue  $\sim 79$  kDa pro-VCC is arranged into four structural domains (Fig. 1): the  $\sim 125$ -residue N-terminus Pro-domain that shows sequence homology to

the Hsp90 family of heat-shock proteins, the  $\sim 250$  amino acid cytotoxin domain that bears similarity to the structure of the cytotoxin domains of other  $\beta$ -PFTs, notably *Staphylococcus aureus*  $\alpha$ -toxin [14] and is central to the structure and function of VCC as a  $\beta$ -PFT [4–6], a  $\sim 116$  amino acid domain related to the carbohydrate-binding domain B of the plant toxin ricin with  $\beta$ -trefoil fold [15] and a  $\sim 140$ -residue domain related to the sugar-binding domain of the plant lectin jacalin with  $\beta$ -prism fold [16]. With the exception of the  $\beta$ -trefoil lectin domain, which has not been studied so far but from indirect evidences is thought to be functionally redundant, all domains have been assigned specific biochemical roles. The Pro-domain locks the assembly of the toxin monomer to the  $\beta$ -barrel by interacting with the cytotoxin domain (Fig. 1) and prevents premature oligomerization [11,13]. The cytotoxin domain mediates oligomerization and membrane penetration [2,13]. The C-terminus  $\beta$ -prism lectin domain mediates targeting of the toxin to cell surface  $\beta 1$ -galactosyl-terminated glycoconjugates [17–20]. Although the domains appear to be discrete structural and functional units (Fig. 1), they profoundly affect the global properties of pro-VCC and VCC by mechanisms not related to their assigned roles. The pro-domain plays a chaperone-like role in regulating folding of the nascent polypeptide to its native conformation and, in absence of the domain, the mature VCC is expressed as functionally inactive aggregates highly

\* Corresponding author.

E-mail address: [kbanerjee51@gmail.com](mailto:kbanerjee51@gmail.com) (K.K. Banerjee).

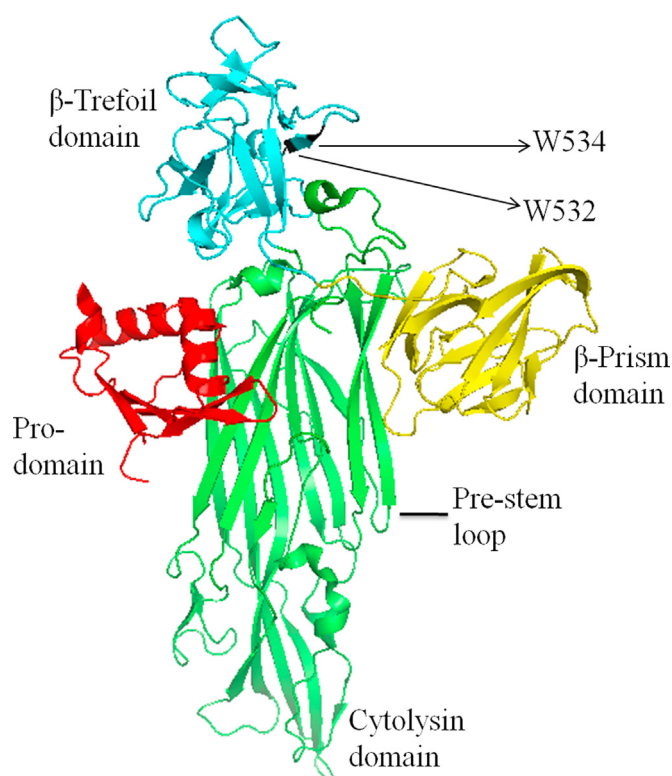


**Fig. 1.** Crystal structure of pro-VCC [13]. Trp532 and Trp534 in the  $\beta$ -trefoil domain selected for point mutation are shown by arrows.

susceptible to proteolytic degradation [21]. Similarly, the cryo-electron microscopy [22] and X-ray crystallography [23] of the membrane-inserted  $\beta$ -barrel VCC heptamer revealed that there is considerable realignment of the  $\beta$ -prism domain relative to the cytolyisin domain during oligomerization. We showed by solution study that the domain promotes VCC assembly to the  $\beta$ -barrel heptamer by making a significant contribution to the entropy of oligomerization [24]. Although deletion of the  $\beta$ -prism domain has no effect on the global conformation of the toxin monomer, the presence of the domain augments the hemolytic activity of VCC by  $\sim 1000$ -fold [17–20,24]. The observations illustrate how discrete domains communicate with each other to increase the functional efficiency of a multidomain protein.

No function has been assigned to the  $\beta$ -trefoil domain, which sits on the top of the cytolyisin domain covering an area of 298 Å at the interface (Fig. 1). Intriguingly, while the  $\beta$ -prism domain with a definite role in pore formation is missing in most of the  $\beta$ -PFTs related to VCC, the  $\beta$ -trefoil domain without an apparent biological function is a recurrent feature of all these toxins [13,25]. In this communication, we have produced VCC variants that either lack the  $\beta$ -trefoil domain or have the domain modified by mutation of Trp532 or Trp534 by Ala. We show that the domain makes a critical contribution to the folding of the hemolytically active conformation of VCC.

## 2. Materials and methods

### 2.1. Preparation of wild-type and mutant toxins: homogeneity and hemolytic activity

The wild-type toxin as well as the mutants were prepared by cloning Pro-VCC [11,13] into the pET32a<sup>+</sup> expression vector (Novagen) and transformed into SHuffle™ T7 competent *Escherichia coli* cells (New England Biolabs). The hexahistidine-tagged pro-

VCC was isolated by chromatography of the cell lysate on Ni<sup>2+</sup>-agarose column. The pro-domain including the histidine tag was removed by trypsinization at an enzyme: substrate ratio of 1:500 at room temperature for 20 min. The mature toxin was purified by hydrophobic interaction chromatography on phenyl-Sepharose CL-4B [24].

The internal  $\beta$ -trefoil lectin domain encoded by the 366 bp long nucleotide sequence was deleted by PCR based mutagenesis. First, a forward (C) and a reverse (B) mutagenic primer encompassing a region of 20 complementary bases not including the sequence to be deleted were designed. Next, a forward VCC primer (A) from the 5' end of the VCC gene containing the BamHI restriction site and a reverse primer (D) from the 3' containing the XhoI restriction site were designed. Two initial PCRs were performed using primer pair A and B together and pair C and D together which gave amplified product of 1377 bp (PCR 1) and 408 bp (PCR 2) respectively. For fusion of the amplified fragments, 1  $\mu$ l product from PCR 1 and 3  $\mu$ l product from PCR 2 were taken together as templates and the PCR was done for 10 cycles without primer. This step produced a nucleotide sequence of 1785 bp joining the two amplified fragments devoid of the  $\beta$ -trefoil gene. The fragment was amplified by using primers A and D and was cloned in pGEM-T Easy Vector System (Promega, USA) using TA cloning method and transformed into JM109 cells. The plasmid was purified from positive colonies screened by PCR, purified and the sequence confirmed by DNA sequencing. Following digestion by BamHI and XhoI, the product was ligated with pET32a<sup>+</sup> vector digested with the same pair of restriction enzymes. The ligated plasmid was transformed into T7 competent cell and the integrity of the pro-VCC $^{\Delta\beta\text{-trefoil}}$  sequence was confirmed by DNA sequencing.

Site-directed mutagenesis was carried out by a PCR-based method by using pET32a<sup>+</sup> plasmid according to the protocols of QuickChangeR Site-Directed Mutagenesis Kit (Stratagene). Primers for the mutation of the two sites in the  $\beta$ -trefoil domain of VCC, viz. Trp532Ala and Trp534Ala were obtained from Sigma Aldrich and the sequences were designed according to the instruction of the manufacturer. The mutation was confirmed by automated DNA sequencing (ABI PRISM 3100). The protein concentration was quantified by a modified Lowry protocol [26] relative to bovine serum albumin as standard. The homogeneity of the protein preparation was monitored by SDS-polyacrylamide gel electrophoresis (SDS-PAGE) in 10% gel [27]. The hemolytic activity was assayed against a 1% suspension of washed rabbit erythrocytes in phosphate-buffered saline (PBS), pH 7.0 following incubation at 25 °C for 1 h.

### 2.2. Monitoring of protease susceptibility

VCC and its mutants were examined for their intrinsic resistance to proteases arising from possessing a folded compact structure by incubating the proteins with trypsin and chymotrypsin at a high enzyme: substrate weight ratio of 1:50 for 15 min at 25 °C. The reactions were terminated by adding an equal volume of 5% trichloroacetic acid. Following incubation at 4 °C for 1 h, the protein precipitates were washed thrice with 9 volumes of cold acetone, dissolved in boiling 10 mM sodium phosphate buffer, pH 7.8 containing 1% SDS and 5% 2-mercaptoethanol and subjected to SDS-PAGE [27].

### 2.3. Triton X-114 partitioning

To see if the mutant toxins possessed a hydrophobic surface similar to the wild-type VCC [28], proteins were dissolved in 2% Triton X-114 (Sigma) at 4 °C and separated into two phases by raising the temperature to 25 °C [29]. Following centrifugation at 10,000  $\times$  g for 10 min at 25 °C, equal volumes of aliquots were

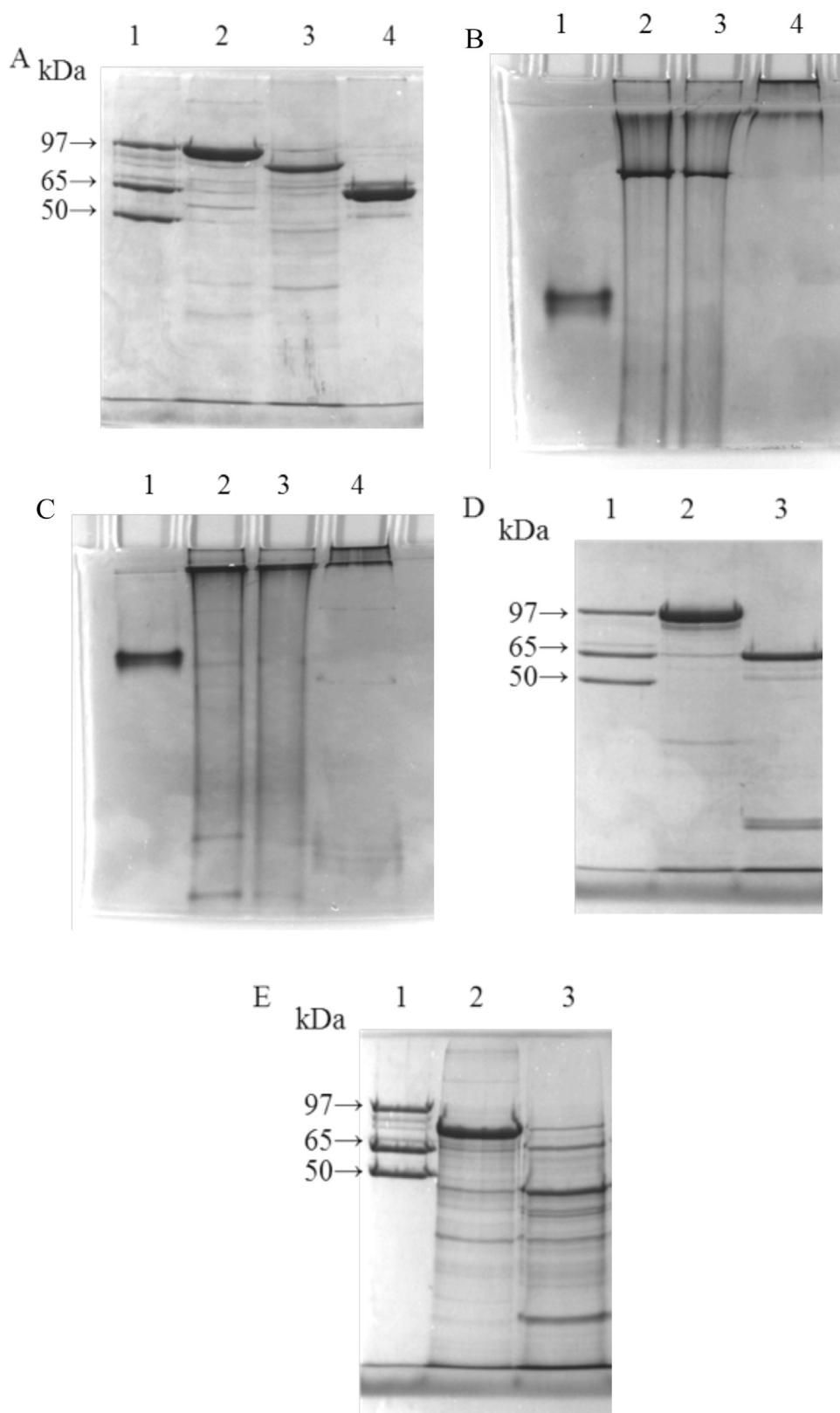


**Fig. 2.** Effect of mutation of the  $\beta$ -trefoil domain on electrophoretic mobility in PAGE. About 4  $\mu$ g of protein was applied to each lane. The gels were stained in Coomassie Brilliant Blue. A, SDS-PAGE in 10% gel of pro-VCC (lane 2), pro-VCC without the  $\beta$ -trefoil domain (lane 3) and VCC (lane 4). A mixture of the three variants of the wild toxin, viz. pro-VCC, VCC and the 50 kDa VCC without the  $\beta$ -prism domain was included as reference (lane 1). PAGE under nonreducing conditions in 6% (B) and 10% (C) gel. Lane 1, VCC; lane 2, VCCW532A; lane 3, VCCW534A; lane 4, pro-VCC mutant without the  $\beta$ -trefoil domain. D and E. Trypsin digestion pattern of pro-VCC and pro-VCC without the  $\beta$ -trefoil domain by SDS-PAGE in 10% gel. Protein (5  $\mu$ g) was incubated with trypsin at an enzyme: substrate weight ratio of 1:500 at 25 °C for 20 min in 50 mM Tris-HCl buffer, pH 8.0 and processed as described in the text. Lane 1, mixture of pro-VCC, VCC and the 50 kDa VCC variant without the  $\beta$ -prism domain; Lane 2, untreated pro-VCC (D) and pro-VCC without the  $\beta$ -trefoil domain (E); Lane 3, trypsin-digested pro-VCC (D) and pro-VCC without the  $\beta$ -trefoil domain (E).

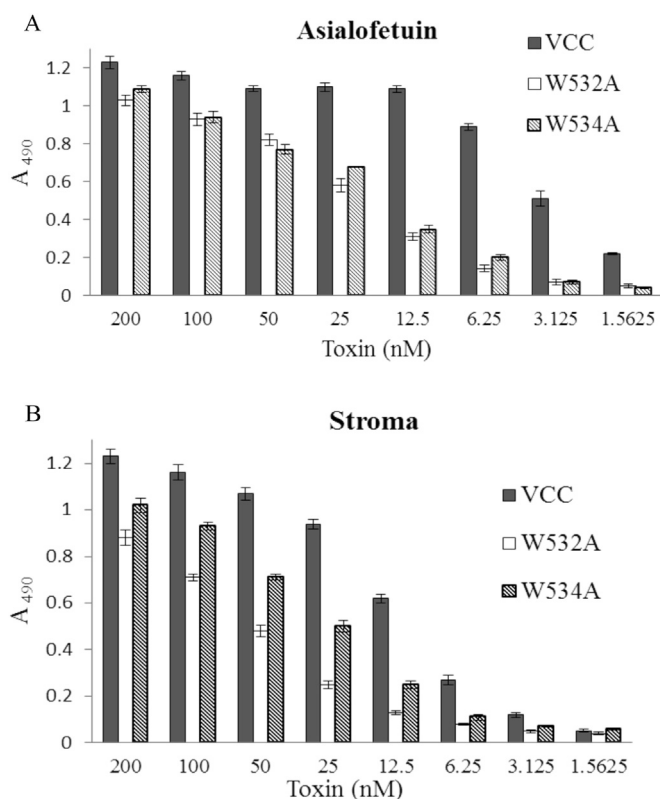


**Fig. 3.** Quantification of the effects of Trp mutation of the  $\beta$ -trefoil domain on carbohydrate-dependent interactions of VCC with asialofetuin (A) and rabbit erythrocyte stroma (B) by ELISA. Each point represents the average of three independent readings with error bars indicating standard deviation.

withdrawn from the water- and detergent-rich phases and treated with 9 volumes of cold acetone. The protein precipitates were dissolved in the presence of SDS and examined by SDS-PAGE [27].

#### 2.4. Quantification of affinity for asialofetuin and rabbit erythrocyte stroma by Enzyme-linked Immunosorbent Assay (ELISA)

Asialofetuin was prepared by treatment of fetuin (Sigma) with neuraminidase (Sigma) in 50 mM sodium acetate-acetic acid buffer, pH 5.0 containing 50 mM  $\text{CaCl}_2$  [30]. Rabbit erythrocyte stroma was prepared by hypotonic lysis of washed erythrocytes with 5 mM sodium phosphate buffer, pH 8.0 at 4 °C. Wells of a 96-well polystyrene plate (Nunc) were coated by overnight incubation with 100  $\mu\text{l}$  of asialofetuin or the stroma suspension (1  $\mu\text{g}$  protein/well) in 50 mM sodium carbonate, pH 9.0. The free sites were blocked by 3 h incubation with 2% defatted milk powder in PBS followed by incubation with the wild or mutant toxin diluted serially in PBS [17,24]. The immobilized toxin was quantified by sequential incubation with rabbit antiserum to VCC diluted 1:500 in PBS, and anti-rabbit IgG conjugated to peroxidase (1:1000, Sigma). Each incubation step was preceded by washing wells with 200  $\mu\text{l}$  of 0.05% Tween-20 in PBS thrice. VCC or its mutants bound to the immobilized glycoprotein or the stroma was quantified by color development with hydrogen peroxide and o-phenylenediamine at 492 nm. Apparent association constants were calculated by KyPlot.

#### 2.5. Transmission electron microscopy

VCCW532A and VCCW534A in PBS were adsorbed on a glow-discharged carbon-coated copper grid, negatively stained with 2% uranyl acetate and examined under a JEOL JEM 1400 transmission

electron microscope (Jeol Ltd., Tokyo, Japan) at 80 kV. Images were analyzed using DIGITAL MICROGRAPH software provided with an Ovis SC200B CCD camera (Gatan, Oxfordshire, UK).

### 3. Results and discussion

#### 3.1. The $\beta$ -trefoil domain was required for correct folding of pro-VCC

Unlike the C-terminus  $\beta$ -prism domain that can be nicked by proteolysis from the rest of the molecule, the  $\beta$ -trefoil domain lying in-between the cytolytic and  $\beta$ -prism domains [2] could not be removed from pro-VCC or VCC by proteolysis. So, we produced the pro-VCC variant without the  $\beta$ -trefoil domain by recombinant DNA technology (lane3, Fig. 2A). In contrast to the wild pro-VCC, which is monodisperse with a molecular weight of 79 K [11], the pro-VCC minus the  $\beta$ -trefoil domain formed large water-soluble aggregate(s) that failed to penetrate the 6% polyacrylamide gel in the absence of SDS (lane 4, Fig. 2B). Limited proteolysis of the wild pro-VCC produced the mature toxin with proteolysis stopping with the cleavage of the Pro-domain; however, the pro-VCC without the  $\beta$ -trefoil domain showed extensive fragmentation under similar conditions of proteolysis (lane 3, Fig. 2E), indicating an open structure with wide accessibility of the peptide bonds to a protease.

#### 3.2. Modification of the $\beta$ -trefoil domain by Trp mutation led to increase in effective size with inactivation of hemolytic activity

Next, we examined if a structurally altered  $\beta$ -trefoil domain affected the folding of pro-VCC. Because Trp has a much larger van der Waals volume (238 Å<sup>3</sup>) in comparison to that of Ala (92 Å<sup>3</sup>) and is also more hydrophobic as well as hydrophilic than Ala [31,32], it seemed likely that the replacement of either Trp532 or Trp534 by Ala would have serious spatial and energetic implications for the conformation of the domain. Accordingly, we selected the two Trp residues for point mutation. Both VCCW532A and VCCW534A appeared to be even more strongly resistant to proteolysis by trypsin and chymotrypsin than the wild toxin (Fig. 4A) indicating that they have compact structures characteristic of a properly folded protein. However, both the Trp mutants showed significantly reduced electrophoretic mobility in 6% (Fig. 2B) and 10% (Fig. 2C) polyacrylamide gels under nonreducing conditions, indicating that they have significantly larger effective hydrodynamic volumes than the wild VCC. VCCW532A and VCCW534A showed 500- and 250-folds, respectively, less hemolytic activity than the wild-type VCC. Both the mutants showed strong hemagglutinating activity toward rabbit erythrocytes without causing hemolysis; interestingly, the behavior of the mutant toxins was reminiscent of that of the renatured wild-type toxin unfolded by urea [34] and indicated a multimeric lectin-like structure.

#### 3.3. Trp mutation of the $\beta$ -trefoil domain caused a marginal decrease in carbohydrate-dependent interaction of VCC

Because the hemolysis is a composite rather than a single event, a drastic decrease in hemolytic activity as a result of the Trp mutation could arguably arise from the inactivation of the initial interaction of the mutant toxins with the erythrocyte surface or abrogation of membrane events like self-assembly and membrane insertion [4–6]. To explore the first possibility, we quantified the binding of the toxin to immobilized asialofetuin (Fig. 3A), a  $\beta$ 1-galactosyl-terminated glycoprotein inhibitor of VCC [17,24] and rabbit erythrocyte stroma (Fig. 3B) by ELISA. In contrast to the total inactivation of carbohydrate-binding activity caused by the



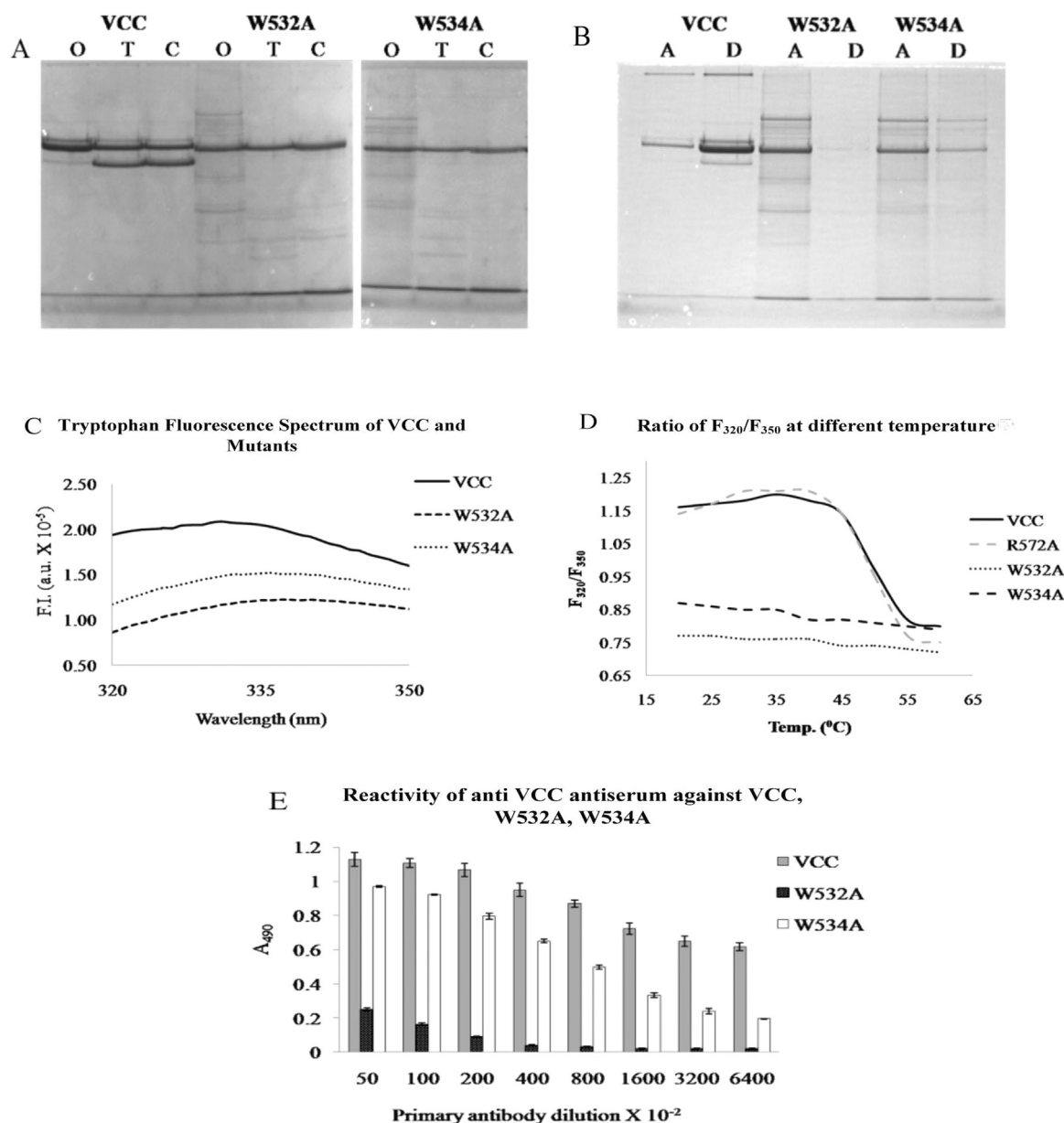


**Fig. 4.** Mutation of the  $\beta$ -trefoil domain and the global conformation of VCC. **A.** Trypsin and chymotrypsin digestion pattern of VCCW532A and VCCW534A. The mutant toxin (5  $\mu$ g) was incubated with trypsin and chymotrypsin at a high enzyme: substrate weight ratio of 1:50 at 25  $^{\circ}$ C for 1 h in 50 mM Tris-HCl buffer, pH 8.0 and processed as described in the text. The protease digestion pattern was analyzed by SDS-PAGE in 10% gel. Lanes O, T and C indicate untreated toxin, toxin treated with trypsin and with chymotrypsin, respectively. **B.** Inversion of surface polarity as a result the Trp mutation the  $\beta$ -trefoil domain detected by Triton X-114 partitioning (See text for details [28]). The water- and detergent-enriched phases are indicated by A and D, respectively. The toxin in the aqueous and detergent phases is visualized by SDS-PAGE in 10% gel. **C.** Intrinsic Trp fluorescence emission spectra of VCC and mutants. The spectra were obtained by exciting a sample of 80  $\mu$ g of purified protein in Tris HCl buffer, pH 8.0 at 295 nm in PTI BasicQuarterMaster 40 spectrofluorimeter (Photon Technology International, UK) and emission spectra were recorded between 320–360 nm. **D.** Temperature-dependent unfolding of wild type and mutant VCC was analyzed by recording Trp fluorescence emission in the temperature range from 20 to 60  $^{\circ}$ C with 5  $^{\circ}$ C increment as described above. The sample was kept for 5 min for equilibration at each temperature in the cuvette before recording of data. The data are presented as the plot of the ratio of emission intensities at 320 and 350 nm  $F_{320}/F_{350}$  vs. temperature. **E.** Reactivity of mouse anti-VCC antiserum with VCC, VCCW532A and VCCW534A. Plates were coated by overnight incubation with 1  $\mu$ g of the toxin followed by serial dilution with mouse anti-VCC antiserum in PBS as described in the text.

deletion of the  $\beta$ -prism domain or mutation of Asp617 [19,20,24], mutations in the  $\beta$ -trefoil domain caused a marginal decrease in the affinity of VCC for asialofetuin and the erythrocyte stroma that corresponded to a decrease in association constant by less than one order of magnitude from  $\sim 3 \times 10^8$  to  $\sim 5 \times 10^7$  M $^{-1}$ . The data suggested that the ricin-like  $\beta$ -trefoil lectin domain did not significantly contribute to the lectin-like interaction of VCC with asialofetuin and stroma; secondly, Trp mutation of the  $\beta$ -trefoil domain had little or no impact on the  $\beta$ -prism domain.

#### 3.4. Mutation of Trp<sup>532</sup> and Trp<sup>534</sup> to Ala Induced Dramatic Conformational Transition of VCC to a New Folded State

The solubility in water and the resistance to proteolysis suggested folded conformations for VCCW532A and VCCW534A. Because the mutants were hemolytically inactive and failed to self-assemble in lipid vesicles (data not shown) but retained carbohydrate-binding activity, they must have conformations different from that of the wild toxins. In contrast to VCC, which had a strongly hydrophobic surface [27], VCCW532A and VCCW534A

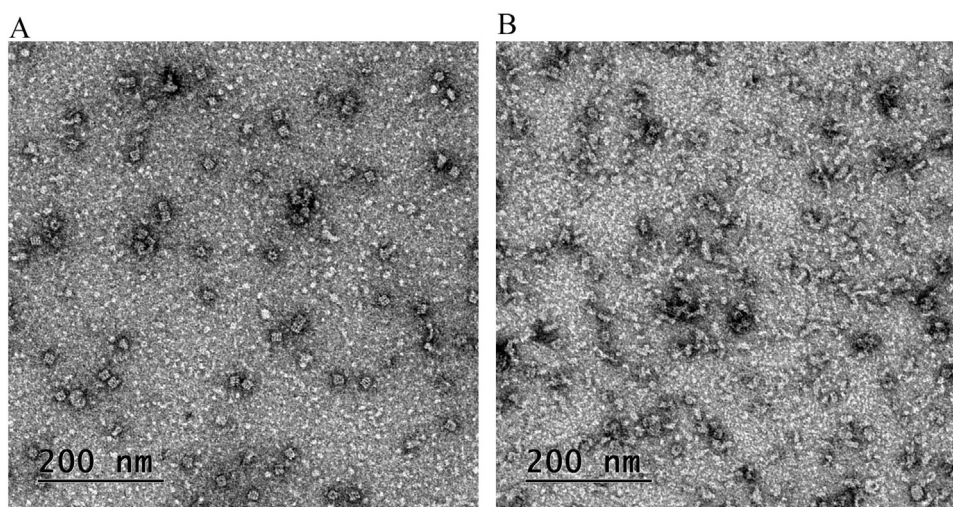


**Fig. 5.** Transmission electron micrographs of negatively stained samples of VCCW532A (A) and VCCW534A (B). Magnification is shown by the scale bar.

(Fig. 4B) moved quantitatively to the aqueous phase in preference to the Triton X-114-enriched phase, suggesting that the mutant proteins had hydrophilic surfaces compatible with the aqueous rather than an amphipathic environment. The intrinsic tryptophan fluorescence emission spectra of the Trp mutants VCCW532A and VCCW534A (Fig. 4C) showed no clear maxima; the ratio of the fluorescence emission intensities,  $F_{320}/F_{350}$ , at 320 and 350 nm, which correspond to the emission maxima in cyclohexane and water, respectively, is 0.77 for VCCW532A and 0.88 for VCCW534A in comparison to a value of 1.21 for the wild-type toxin. It appears that Trp residues in the mutant toxins moved from the hydrophobic core of the protein to the surface. The plot of  $F_{320}/F_{350}$  for the Trp mutants over the temperature range from 20 to 60 °C did not show any indication of a thermal transition in contrast to the sharp transition to the unfolded state shown by the wild-type toxin at around 50 °C (Fig. 4D; [24]). Due to a unique combination of hydrophobicity and hydrophilicity, Trp is adapted to exist in the protein core as well as on the protein-water interface [31,32]; therefore, absence of a Trp fluorescence emission maximum (Fig. 4C) does not necessarily indicate unfolding. In contrast to the dramatic change introduced by Trp mutation in the global conformation, substitution of the polar Arg272 by alanine had no effect on the fluorescence emission spectrum (Fig. 4D).

Antibodies raised against a native protein contain a population that is specific for the surface epitopes of the folded conformation and, so, can be used as probes to monitor conformational changes [33]. Because inversion of the surface polarity and spectrofluorimetric data suggested that at least a significant proportion of the surface epitopes characteristic of the wild toxin should be missing in the Trp mutants, we expect that the antiserum to the wild-type toxin would distinguish between the wild-type and mutant toxins. The rabbit anti-VCC polyclonal antiserum indeed showed considerably lower affinity for the Trp mutants than for the wild toxin (Fig. 4E).

### 3.5. VCCW532A and VCCW534A are ring-shaped molecules

Previously, we observed that the transmission electron micrograph of the wild-type VCC monomer failed to reveal a distinguishing morphology, presumably due to the limited resolving power of the electron microscope in comparison to the X-ray crystallography. The VCC heptamer formed in the membrane lipid bilayer or liposomes showed ring-like molecules of diameter ~10 nm with the seven monomers arranged with circular symmetry at the periphery of a central hollow [22,24]. The

transmission electron micrographs of aqueous suspensions of VCCW532A (Fig. 5A) and VCCW534A (Fig. 5B) showed morphological similarities to the  $\beta$ -barrel VCC heptamer [22,24]. The rings appeared to be uniform in shape; however, unlike the  $\beta$ -barrel heptamer, they were SDS-labile and were significantly larger with mean diameters of ~19 nm. Furthermore, the mutant rings tended to stack as cylinders of varying heights in contrast to the lateral aggregates formed by the VCC  $\beta$ -barrel heptamers in the absence of detergents.

### 3.6. Conclusion

The present study shows that the folding of the pro-VCC polypeptide to its so-called native conformation is critically dependent on the  $\beta$ -trefoil domain. It appears, in retrospect, that the hemolytically active conformation is unusually sensitive to minor perturbation, e.g. nondenaturing concentrations of urea (~2 M) trigger switchover to an inactive aggregate that retains carbohydrate-binding activity suggesting that the so-called native conformation of VCC might not be the most stable arrangement of the protein [34]. It is tempting to compare the role of the  $\beta$ -trefoil domain with that of the Pro-domain, which is also required for folding of the VCC polypeptide to the  $\beta$ -PFT [21]. In comparison, the  $\beta$ -prism lectin domain is an autonomous folding unit with no requirement for the Pro- or the  $\beta$ -trefoil domain. The role of the N-terminus Pro-domain is restricted to protein folding and does not extend to its post-folding functioning. Since we could not cleave off the internal  $\beta$ -trefoil domain, we are not sure if its role is limited to regulating folding or extends to the post-folding functioning of the toxin.

### Funding

This research did not receive any specific grant from funding agencies in the public, commercial, or not-for-profit sectors.

### Conflict of interest

Authors declare that they have no conflict of interest with the content of this manuscript.

## Author's contributions

A. M. designed and performed most of the experiments. All authors contributed to designing, performing and interpreting experiments. K.K.B. conceived the study, interpreted the experiments and wrote the paper. All authors agree to the content of the manuscript.

## Acknowledgement

We gratefully acknowledge the help of A. N. Ghosh, National Institute of Cholera and Enteric Diseases, Kolkata, India and Kalyan Mitra, Central Drug Research Institute, Lucknow, India in the transmission electron microscopy work. We thank Subrata Sabui, University of California, Irvine for useful discussion.

## Appendix A. Transparency document

Transparency document associated with this article can be found in the online version at <http://dx.doi.org/10.1016/j.bbrep.2016.09.009>.

## References

- [1] A. Zitzer, I. Walev, M. Palmer, S. Bhakdi, Characterization of *Vibrio cholerae* cytotoxin as an oligomerizing pore-forming toxin, *Med. Microbiol. Immunol.* 184 (1995) 37–44.
- [2] R. Olson, E. Gouaux, *Vibrio cholerae* cytotoxin is composed of an  $\alpha$ -hemolysin-like core, *Protein Sci.* 12 (2003) 379–383.
- [3] A.K. Rai, K. Chattopadhyay, *Vibrio cholerae* cytotoxin: structure-function mechanism of an atypical  $\beta$ -barrel pore-forming toxin, in: A. Chakraborty, A. Suroli (Eds.), *Biochemical Roles of Eukaryotic Cell Surface Macromolecules*, 842, Springer International Publishing Switzerland, 2015, Chapter 7, 109–125.
- [4] A.P. Heuck, R.K. Tweten, A.E. Johnson,  $\beta$ -Barrel pore-forming toxins: intriguing dimorphic proteins, *Biochemistry* 40 (2001) 9063–9065.
- [5] R.J.C. Gilbert, Pore-forming toxins, *Cell. Mol. Life Sci.* 59 (2002) 832–844.
- [6] M.D. Peraro, F.G. van der Goot, Pore-forming toxins: ancient, but never really out of fashion, *Nat. Rev. Microbiol.* 14 (2016) 77–92.
- [7] O.V. Krasilnikov, J.N. Muratkodjaev, A. Zitzer, The mode of action of *Vibrio cholerae* cytotoxin: the influences on both erythrocytes and planar lipid bilayers, *Biochim. Biophys. Acta* 1111 (1992) 7–16.
- [8] H.K. Saka, C. Bidinost, C. Sola, P. Carranza, C. Collino, S. Ortiz, J.R. Echenique, J. L. Bocco, *Vibrio cholerae* cytotoxin is essential for high enterotoxicity and apoptosis induction produced by a cholera toxin gene-negative *V. cholerae* non-O1, non-O139 strain, *Microb. Pathog.* 44 (2008) 118–128.
- [9] D.C. Chakraborty, G. Mukherjee, P. Banerjee, K.K. Banerjee, T. Biswas, Hemolysin induces Toll-like receptor (TLR)-independent apoptosis and multiple TLR-associated parallel activation of macrophages, *J. Biol. Chem.* 286 (2011) 34542–34551.
- [10] J.B. Kaper, J.G. Jr Morris, M.M. Levine, Cholera, *Clin. Microbiol. Rev.* 8 (1995) 48–86.
- [11] K. Yamamoto, Y. Ichinose, H. Shinagawa, K. Makino, A. Nakata, M. Iwanaga, T. Honda, T. Miwatani, Two-step processing for activation of the cytotoxin/hemolysin of *Vibrio cholerae* O1 biotype El Tor: nucleotide sequence of the structural gene (hlyA) and characterization of the processed products, *Infect. Immun.* 58 (1990) 4106–4116.
- [12] K.J. Fullner, J.C. Boucher, G.K. Hanes, G.K. Hanes 3rd, B.M. Meehan, C. Walchle, P.J. Sansonetti, J.J. Mekalanos, The contribution of accessory toxins of *Vibrio cholerae* O1 El Tor to the proinflammatory response in a murine pulmonary cholera model, *J. Exp. Med.* 195 (2002) 1455–1462.
- [13] R. Olson, E. Gouaux, Crystal structure of the *Vibrio cholerae* cytotoxin (VCC) protoxin and its assembly into a transmembrane pore, *J. Mol. Biol.* 350 (2005) 997–1016.
- [14] L. Song, M.R. Hobaugh, C. Shustak, S. Cheley, H. Bayley, E. Gouaux, Structure of staphylococcal  $\alpha$ -hemolysin, a heptameric transmembrane pore, *Science* 274 (1996) 1859–1866.
- [15] W. Montfort, J.E. Villafranca, A.F. Monzingo, S.R. Ernst, B. Katzin, E. Rutenber, N. H. Xuong, R. Hamlin, J.D. Robertus, The three-dimensional structure of ricin at 2.8 Å, *J. Biol. Chem.* 262 (1987) 5398–5403.
- [16] R. Sankaranarayanan, K. Sekar, R. Banerjee, V. Sharma, A. Suroli, M. Vijayan, A novel mode of carbohydrate recognition in jacalin, a *Moraceae* plant lectin with a  $\beta$ -prism fold, *Nat. Struct. Biol.* 3 (1996) 596–603.
- [17] N. Saha, K.K. Banerjee, Carbohydrate-mediated regulation of interaction of *Vibrio cholerae* hemolysin with erythrocyte and phospholipid vesicle, *J. Biol. Chem.* 272 (1997) 162–167.
- [18] B. Mazumdar, S. Ganguly, A.N. Ghosh, K.K. Banerjee, The role of C-terminus carbohydrate-binding domain of *Vibrio cholerae* hemolysin/cytotoxin in the conversion of the pre-pore  $\beta$ -barrel oligomer to a functional diffusion channel, *Indian J. Med. Res.* 133 (2011) 131–137.
- [19] S. Levan, S. De, R. Olson, *Vibrio cholerae* cytotoxin recognizes the hepta-saccharide core of complex N-glycans with nanomolar affinity, *J. Mol. Biol.* 425 (2013) 944–947.
- [20] A.K. Rai, K. Paul, K. Chattopadhyay, Functional mapping of the lectin activity site on the  $\beta$ -prism domain of *Vibrio cholerae* cytotoxin. Implication for the membrane pore formation mechanism of the toxin, *J. Biol. Chem.* 288 (2013) 1665–1673.
- [21] K. Nagamune, K. Yamamoto, T. Honda, Intramolecular chaperone-like activity of the Pro-region of *Vibrio cholerae* El Tor cytotoxin, *J. Biol. Chem.* 272 (1997) 1338–1343.
- [22] S. Dutta, B. Mazumdar, K.K. Banerjee, A.N. Ghosh, Three-dimensional structure of different forms of the *Vibrio cholerae* hemolysin oligomer: a cryo-electron microscopic study, *J. Bacteriol.* 192 (2010) 169–178.
- [23] S. De, R. Olson, Crystal structure of the *Vibrio cholerae* cytotoxin heptamer reveals common features among disparate pore-forming toxins, *Proc. Natl. Acad. Sci. USA* 108 (2011) 7385–7390.
- [24] S. Ganguly, A. Mukherjee, B. Mazumdar, A.N. Ghosh, K.K. Banerjee, The  $\beta$ -prism lectin domain of *Vibrio cholerae* hemolysin promotes self-assembly of the  $\beta$ -pore-forming toxin by a carbohydrate-independent mechanism, *J. Biol. Chem.* 289 (2014) 4001–4008.
- [25] K. Kaus, J.W. Lary, J.L. Cole, R. Olson, Glycan specificity of the *Vibrio vulnificus* hemolysin lectin outlines evolutionary history of membrane targeting by a toxin, *J. Mol. Biol.* 426 (2014) 2800–2812.
- [26] M.A.K. Markwell, S.M. Haas, L.L. Bieber, N.E. Tolbert, A modification of the Lowry procedure to simplify protein determination in membrane and lipoprotein samples, *Anal. Biochem.* 87 (1978) 206–210.
- [27] U.K. Laemmli, Cleavage of structural proteins during the assembly of the head of the head of bacteriophage T4, *Nature* 227 (1970) 680–685.
- [28] K. Chattopadhyay, D. Bhattacharyya, K.K. Banerjee, *Vibrio cholerae* hemolysin: Implication of amphiphilicity and lipid-induced conformational change for its pore-forming activity, *Eur. J. Biochem.* 269 (2002) 4351–4358.
- [29] C. Bordier, Phase separation of integral membrane proteins in Triton X-114 solution, *J. Biol. Chem.* 256 (1981) 1604–1607.
- [30] R.G. Spiro, Studies of fetuin, a glycoprotein of fetal serum. Isolation, chemical composition and physicochemical properties, *J. Biol. Chem.* 235 (1960) 2860–2869.
- [31] C. Chothia, The nature of the accessible and buried surfaces in proteins, *J. Mol. Biol.* 105 (1976) 1–14.
- [32] A. Radzicka, R. Wolfenden, Comparing the polarities of the amino acids: side-chain distribution coefficients between the vapor phase, cyclohexane, 1-octanol and neutral aqueous solution, *Biochemistry* 27 (1988) (1988) 1664–1670.
- [33] D.H. Sachs, A.N. Schechter, A. Eastlake, C.B. Anfinsen, An immunologic approach to the conformational equilibria of polypeptides, *Proc. Natl. Acad. Sci. USA* 69 (1972) 3790–3794.
- [34] K. Chattopadhyay, K.K. Banerjee, Unfolding of *Vibrio cholerae* hemolysin induces oligomerization of the toxin monomer, *J. Biol. Chem.* 278 (2003) 38470–38475.